Wavelength-multiplexed phase-locked laser diode interferometer using a phase-shifting technique

Takamasa Suzuki, Takaya Muto, Osami Sasaki, and Takeo Maruyama

We propose a new signal-processing method for eliminating measurement errors that occur in the wavelength-multiplexed phase-locked laser diode interferometer. The basic idea proposed here is a very simple but effective way to improve measurement accuracy. With our scheme, the phase in the interference signal is strictly shifted by 2π, which enables us to eliminate measurement errors. The equivalent wavelength Λ is 80 mm, and the measurement accuracy reaches $\sim\Lambda/600$. A step-height measurement was also carried out in the experiment.

Key words: Interferometer, laser diode, phase lock, equivalent wavelength.

1. Introduction

Optical interferometry is useful in the precise measurement of microscopic vibration or surface roughness, because it is highly sensitivity and does not require physical contact. These days, many kinds of optical interferometers employing a laser diode (LD) have been proposed and are in practical use, but the measurable range of the conventional interferometers is limited by phase ambiguity caused by phase wrapping. To solve this problem, we need devices that perform well in optical systems or in signal processing. One such device is a wavelength-multiplexing method for an optical system. This idea was proposed in the early days of holographic interferometry,[1] but many kinds of two-wavelength interferometers (TWI's) have been proposed[2–4] since then.

Recently, many kinds of LD's have been developed, and they offer many different wavelengths. Therefore TWI's that utilize two different LD's are often proposed.[5–7] The LD is small in size and has some attractive features, such as wavelength tunability and energy efficiency; thus it is suitable for this kind of interferometer. Usually, two different LD's are used in the TWI to obtain two different wavelengths. This type of TWI, however, is necessary to align the optical axes of each LD and to stabilize the relative change in wavelengths.[8] To overcome these problems, a TWI with a single LD has been proposed[9] in which temporally multiplexed wavelengths were used and the phase was detected by the heterodyne method by using an acousto-optic Bragg cell.

On the other hand, we proposed a new type of TWI that used a single LD, and we analyzed its error sources.[10] In that TWI a single LD is oscillated alternately with two wavelengths that are slightly different. The initial phase in the interference signal corresponding to each wavelength is locked at each stable point by using a phase-locked technique.[11–13] The error analysis clarified that a major error source other than external disturbance induced by unknown vibration was offset voltage caused by the total offset voltage of electrical devices in the feedback control system.

In this paper, we introduce a new type of signal processing for feedback control. It is a simple but effective way to eliminate influence from the offset voltage generated by electrical devices. This TWI enables us to measure absolute distance more accurately compared with the TWI that we previously proposed.[10] The external disturbance is also eliminated by feedback control[12,14] and a differential detection.[15] Thus measurement accuracy reaches $\sim\Lambda/600$. A step-height measurement was also carried out in the experiment.

In Section 2 we describe the construction of this interferometer and briefly the principle of wavelength-multiplexed interferometry. A detailed explanation

The authors are with Faculty of Engineering, Niigata University, 8050 Ikarashi 2, Niigata 950-21, Japan.

Received 3 June 1996; revised manuscript received 17 October 1996.

0003-6935/97/256196-06$10.00/0

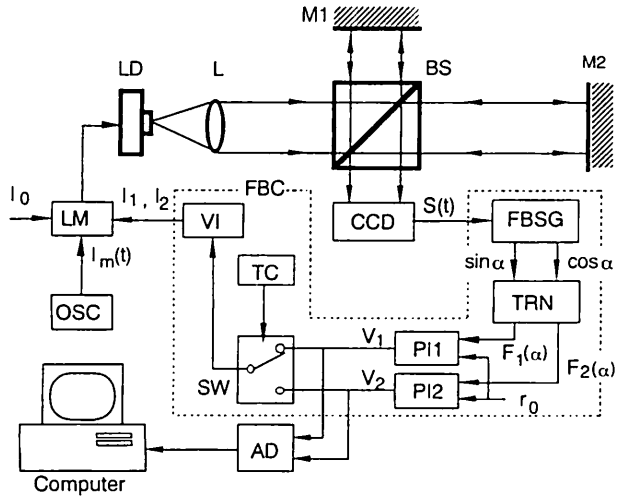

Fig. 1. Experimental setup of the wavelength-multiplexed phase-locked LD interferometer by using a phase-shifting technique. Feedback current I_1 or I_2 generated by the feedback controller (FBC) is injected into the LD through the LD modulator (LM). The FBC consists of a feedback signal generator (FBSG), a feedback signal transition controller (TRN), two PI controllers, a timing controller (TC), a switch (SW), and a voltage-to-current converter (VI). OSC, oscillator.

of eliminating errors introduced by the offset voltage is described in Section 3. The experimental setup and results and discussion are in Sections 4 and 5, respectively.

2. Principle of Wavelength-Multiplexed Interferometry

The configuration of our TWI is shown in Fig. 1. A Twyman–Green interferometer consisting of a LD; a lens, L; a beam splitter, BS; mirrors M1 and M2; and a CCD image sensor are used in the optical system. The optical path difference (OPD) is $2D_0(x)$ in this interferometer, where x denotes the coordinate along the one-dimensional CCD image sensor. A dc bias current I_0, a sinusoidal modulating current,

$$I_m(t) = a\cos(\omega_c t + \theta), \tag{1}$$

and control current I_1 or I_2 is injected into the LD with a laser diode modulator (LM). The control currents, I_1 and I_2, are served alternately from the FBC. The FBC consists of a FBSG; a TRN; two proportional-integral controllers, PI1 and PI2; a SW; a TC; and a VI. The parameter r_0 is the desired value of the control system. The central wavelength λ_0 is determined by I_0. If the control current is zero, an interference signal imaged onto the CCD image sensor is given by

$$S(t, x) = S_1 + S_0\cos[z\cos(\omega_c t + \theta) + \alpha(x)], \tag{2}$$

where

$$z = 4\pi a\beta D_0/\lambda_0^2 \tag{3}$$

is the modulation depth and

$$\alpha(x) = 4\pi D_0(x)/\lambda_0 \tag{4}$$

is the initial phase of the interference signal. S_1 and S_0 are the dc component and the amplitude of the ac component, respectively, and β is the modulating efficiency of the LD. If the LD oscillates with different wavelengths, λ_1 or λ_2, the phase given by Eq. (4) changes slightly as follows:

$$\alpha_1(x) = 4\pi D_0(x)/\lambda_1, \tag{5}$$

$$\alpha_2(x) = 4\pi D_0(x)/\lambda_2, \tag{6}$$

where $\lambda_i = \lambda_0 + \beta I_i = \lambda_0 + \beta K_i V_i$ $(i = 1, 2)$, V_i are the outputs of PI1 and PI2, K_i is the gain of the VI. The phase difference between $\alpha_1(x)$ and $\alpha_2(x)$ is given by

$$\Delta\alpha(x) = 4\pi D_0(x)/\Lambda, \tag{7}$$

where

$$\Lambda = \lambda_1\lambda_2/(\lambda_1 - \lambda_2) \tag{8}$$

is the equivalent wavelength. Then absolute distance $D_0(x)$ is given by

$$D_0(x) = \frac{\Lambda}{4\pi}\Delta\alpha(x). \tag{9}$$

By using control voltages, we rewrite Eq. (9) as

$$D_0(x) = C\frac{\Delta\alpha(x)}{\Delta V}, \tag{10}$$

where $C \approx \lambda_0^2/4\pi\beta K_V$, $\Delta V = V_1 - V_2$. Phases $\alpha_1(x)$ and $\alpha_2(x)$ are locked at specified values by controlling injection currents I_1 and I_2 by a phase-locked technique. Differences $\Delta\alpha$ and ΔV are then determined accurately, and absolute distance $D_0(x)$ can be obtained.

The CCD image sensor is read out every quarter period of the modulation current. Therefore we obtain four integral values:

$$p_i(x) = \int_{(i-1)T/4}^{iT/4} S(t, x)\mathrm{d}t \qquad (i = 1 \sim 4), \tag{11}$$

where $T = 2\pi/\omega_c$ is a period of the modulation current. Signal $p_i(x)$ is sampled and additions and subtractions are executed for $p_i(x)$ in the FBSG. Then we can obtain feedback signals[10]

$$F_s[\alpha(x)] = p_1 + p_2 - p_3 - p_4 = A_s\sin\alpha(x), \tag{12}$$

$$F_c[\alpha(x)] = p_1 - p_2 + p_3 - p_4 = A_c\sin\alpha(x), \tag{13}$$

where A_s and A_c are functions of both modulation depth z and initial phase θ of the modulation current.

3. Error-Reduction Method

Figure 2 shows the feedback signals used in our TWI. In the previous method[10] we used two feedback signals, $F_1(\alpha)$ and $F_2(\alpha)$, whose phase difference was π, as shown in Fig. 2(a), where coordinate x is omitted to simplify the following explanations. In this case, feedback signal $F_1(\alpha)$ is primitive, because the second feedback signal $F_2(\alpha)$ is generated by inverting only

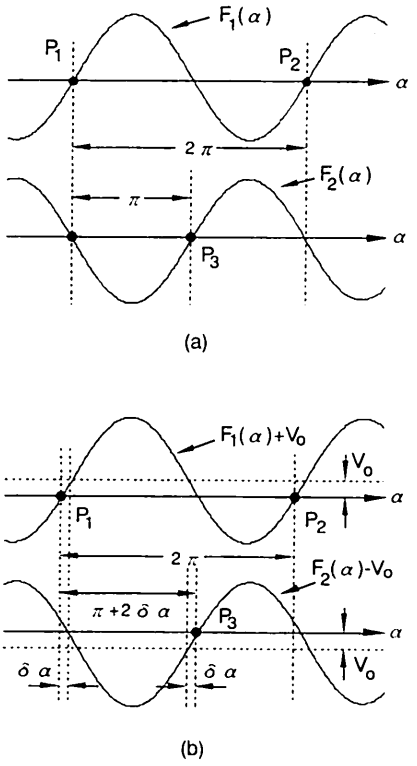

Fig. 2. Feedback signals in (a) the ideal case and (b) the actual case that contains offset voltage V_O. Although the phase difference between P_1 and P_3 in (b) becomes larger than that in (a), the phase difference between P_1 and P_2 is the same in both cases.

$F_1(\alpha)$. Because the phase was controlled at each stable point, P_1 and P_3, which are intersections between the ground level and the region of positive inclination on the feedback signal, phase difference $\Delta\alpha$ was π. This previous method, however, contained one problem or the generation of the measurement error caused by the offset voltage. From a theoretical analysis,[10] we clarified that the offset voltage appears only in the feedback signal sin α by the intensity modulation in the LD. But some offset voltage was observed experimentally also in the feedback signal cos α. We concluded that the offset voltage in the feedback signal cos α came from the electrical circuit. If primitive feedback signal $F_1(\alpha)$ contains positive offset voltage V_O, the negative offset voltage is contained in the second feedback signal $F_2(\alpha)$ as shown in Fig. 2(b). Then phase difference $\Delta\alpha$ becomes larger than π by $2\delta\alpha$, which induces a measurement error.

If the phase of the feedback signal changes periodically, we can distinguish the offset voltage in the electric circuit from the required feedback signal, and we can remove it electrically. But the phase of the feedback signal is a function of the coordinate on the CCD image sensor, and the feedback signal does not change periodically. So electrical cancellation of the offset voltage is impossible.

We proposed here a way to reduce measurement errors caused by offset voltage. Our idea for error reduction is very simple: Phase locks are achieved on the same feedback signal $F_1(\alpha)$ as shown in Fig. 2(a). Then the phase difference $\Delta\alpha$ between the stable points, P_1 and P_2, becomes 2π. In this case, the phase difference $\Delta\alpha$ is accurately 2π even if the offset voltage remains on the feedback signal as shown in Fig. 2(b). Moreover the equivalent wavelength Λ becomes half of that in the previous paper, because $\Delta\alpha$ doubles in Eq. (9). When the same feedback signals are used as $F_1(\alpha)$ and $F_2(\alpha)$, however, two phases are locked at the same stable point, for example, P_1. Therefore we must shift one phase to another stable point, P_2, leaving the other at P_1. It is difficult to move the phase by 2π at one time, without the stability of the control system deteriorating. Therefore the phase should be moved gradually.

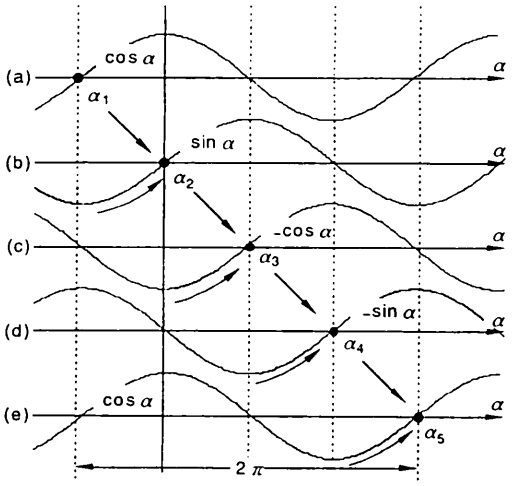

Fig. 3. Phase-shifting process according to the transition of feedback signal $F_2(\alpha)$. Only the transition of feedback signal $F_2(\alpha)$ is shown.

To achieve this process, we use cos α and sin α as primitive feedback signals. Since there is a phase difference of $\pi/2$ between them, we can shift the phase by $\pi/2$. Such feedback signals are obtained easily from the output signal of the CCD image sensor[10] as shown in Eqs. (12) and (13). The proposed procedure is shown in Fig. 3. Only changes in feedback signal $F_2(\alpha)$, while another feedback signal $F_1(\alpha)$ is always cos α, are shown.

In the first stage shown in Fig. 3(a), cos α is commonly used as feedback signals $F_1(\alpha)$ and $F_2(\alpha)$. Then two phases are locked α_1 at the same stable point, P_1, on the feedback signals shown in Fig. 2. In the second stage, $F_2(\alpha)$ changes from cos α to sin α as shown in Fig. 3(b) and the phase moves to α_2. In the third stage, we use $-\cos\alpha$ as feedback signal $F_2(\alpha)$ as shown in Fig. 3(c). Then the phase is moved gradually from α_2 to α_3. In this way, the phase is changed by $\pi/2$ in phase for each step. Finally, in the fifth stage, $F_2(\alpha)$ returns to the initial feedback signal cos α as shown in Fig. 3(e), and the phase settles at the desired stable point, P_2. Therefore the phase difference becomes 2π at the final stage.

4. Experimental Setup

The experimental setup is shown in Fig. 1. The optical path difference $2D_0$ of the Twyman–Green in-

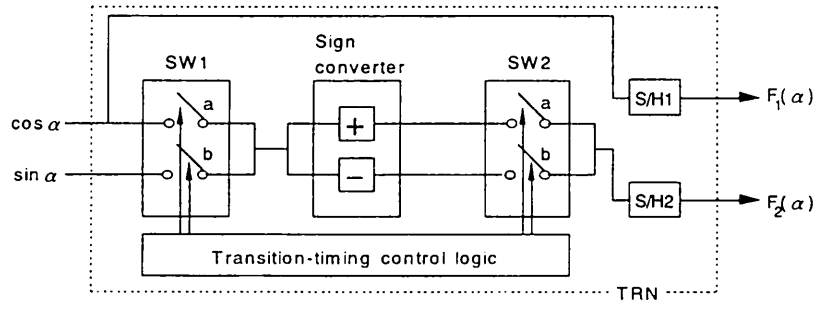

Fig. 4. Block diagram of the feedback signal transition controller TRN. It consists of two analog switches, SW1 and SW2; a sign converter; transition-timing control logic; and two sample-hold circuits, S/H1 and S/H2.

terferometer is ~80 mm. A GaAlAs laser diode is used as a light source. Its maximum output power and central wavelength λ_0 are 5 mW and 780 nm, respectively. The modulation efficiency β of the LD is 6.8×10^{-3} nm/mA. The frequency of the phase modulation $\omega_C/2\pi$ was set to 2 kHz. The interval of the photodetector and the readout frequency of the CCD image sensor are 14 μm and 2 MHz, respectively. The TC determines the switchover period of the feedback signals, $F_1(\alpha)$ and $F_2(\alpha)$. It alternately changes the two feedback signals every 20 periods of the modulation current, i.e., the feedback signal is changed every 10 ms. Because the integral time of the integrator in the PI controller is 3.9 ms, 10 ms is sufficient time for the phase lock to settle. The coefficient K_V is 0.17 mA/V. The desired value r_0 was set to zero to control the phase at the most appropriate position at which the inclination or the gain of the feedback signal is maximum. The control voltages are sampled by the analog-to-digital converter (AD), and $D_0(x)$ is calculated from Eq. (10). Because the phase difference $\Delta\alpha$ is set to 2π in this experiment, the equivalent wavelength Λ was calculated as 80 mm from Eq. (9).

One of the most significant parts of Fig. 1 is a TRN that controls the transition of the feedback signals. A block diagram of the TRN is shown in Fig. 4. It consists of two analog switches, SW1 and SW2; a sign converter; two sample-hold circuits, S/H1 and S/H2; and a transition-timing control logic. The feedback signal, $F_1(\alpha) = \cos\alpha$, is always fed into PI1, whereas the changing feedback signal, $F_2(\alpha)$, is fed into PI2. One of two switches in SW1 and one of two in SW2 are closed to fulfill the sequence shown in Fig. 3. SW1 and SW2 select one feedback signal and the sign of the feedback signal, respectively. To obtain feedback signal sin α in Fig. 3(b), for example, the transition-timing control logic switches on SW1b and SW2a. S/H1 holds $F_1(\alpha)$ until feedback signal $F_2(\alpha)$ is obtained in the FBSG.

5. Experimental Results

First, the control voltages corresponding to Fig. 3 are observed when small external vibrations are added. They are shown in Fig. 5. The lower traces are obtained with $F_1(\alpha)$. In the first stage, the two feedback signals are the same; they are the cos α's shown in Fig. 3(a). The evolutions of two control voltages completely overlap each other, as shown in Fig. 5(a). When one feedback signal $F_2(\alpha)$ is changed from cos α to sin α in the second stage, the difference voltage ΔV appears between the control voltages as shown in Fig. 5(b).

As one feedback signal is being changed in order, such as from sin α to $-\cos\alpha$ and from $-\cos\alpha$ to $-\sin\alpha$, the difference ΔV between two control voltages becomes large. The increased voltage should be the same theoretically at each stage, but it is not the same. This is mainly caused by the offset voltage in sin α discussed in Section 3. The feedback signal sin

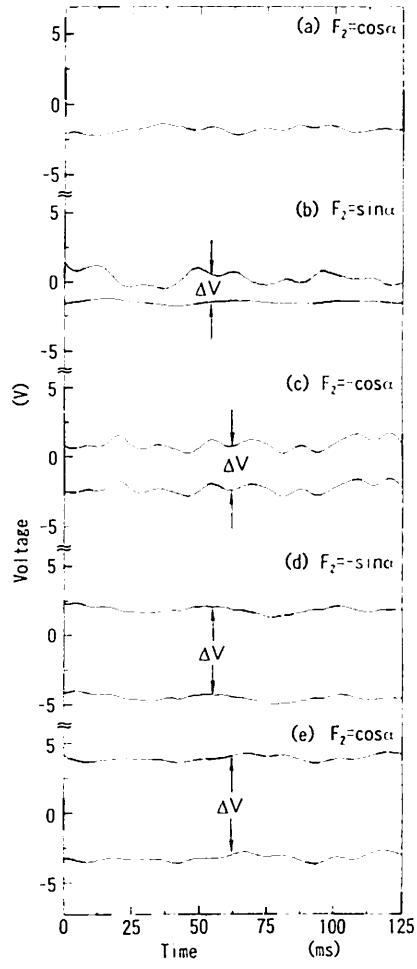

Fig. 5. Observed control voltages corresponding to the feedback signal shown in Fig. 3. The difference ΔV becomes large as the feedback signal is changed.

α theoretically contains an offset component induced by the intensity modulation[10] in the LD, whereas the feedback signal cos α does not contain such an offset component.

The fluctuation was observed in ΔV only in Fig. 5(b). We consider that the offset voltage or the remaining electrical resistance after the switch is closed in the FBC in Fig. 1 generated the error voltage, and it contributed to the fluctuation of ΔV, because the voltage level of the upper trace was almost zero and the signal-to-noise ratio was not as good. But this fluctuation is not as large, and the following controls in Fig. 5 do not suffer. Besides the errors from this source are eliminated with our method, because the phase-lock is achieved by the same feedback signal at the final stage. This is not a fatal error in our system.

ΔV that appeared at the second stage or in Fig. 5(b) is smaller than expected, indicating that the phase difference between $F_1(\alpha)$ and $F_2(\alpha)$ is smaller than $\pi/2$. In this case, the locked phase $\alpha 2$ in Fig. 3(b) is shifted left. Therefore it is obvious that the feedback signal sin α had a positive offset voltage. On the contrary, ΔV that appeared at the fourth stage or in Fig. 5(d) is larger than expected, indicating that the phase difference is larger than $\pi/2$, and the locked phase $\alpha 4$ in Fig. 3(d) was shifted right by the negative offset voltage. Therefore the difference voltage ΔV in Fig. 5(d) is not exactly double that in Fig. 5(b).

On the other hand, the difference in voltage ΔV that appeared in the final stage or in Fig. 5(e) almost doubles compared with that in Fig. 5(c), because the phase difference in the feedback signals in Fig. 5(e) is twice as large as that in Fig. 5(c). It shows that the feedback signal cos α does not contain much offset voltage. The time required from the initial stage in Fig. 5(a) to the final stage Fig. 5(e) is 40 ms.

Next we investigated measurement accuracy by measuring the displacement of mirror M2. The mirror was mounted on the x-axis stage and moved along the optical axis from $D_0 \sim 42$ mm to ~47.5 mm in discrete 0.5-mm increments with a micrometer. Measurements were implemented by keeping the phase difference at 2π. Difference voltage ΔV was detected by subtracting one feedback signal from the other. Then the external disturbance was removed sufficiently. The measured result is shown in Fig. 6. The experimental values agree quite well with the theoretical line. The standard deviation from the theoretical line is 0.12 mm rms. The accuracy of the absolute distance measurement is therefore concluded to be $\sim\Lambda/600$ experimentally. This high accuracy was achieved with double error-reducing techniques, that is, feedback control[12,14] and differential detecting techniques.[15]

Finally, we measured the one-dimensional step height. The object was a block gauge whose thickness was ~2 mm. The measured result is shown in Fig. 7. Circles show the measured values, and they are interpolated with a solid line. The distance was measured along the x axis on the surface of the object

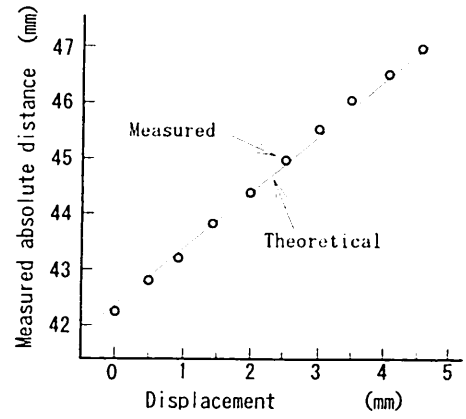

Fig. 6. Measured absolute distance. The object mirror M2 was moved in discrete 0.5-mm increments.

in discrete 14-μm increments. The step height was accurately measured in this interferometer. The measurement error along the x axis was 0.16 mm rms.

With this interferometer, we used the wavelength tunability of the LD. But the current range in which we can obtain a linear wavelength change is restricted to ~10 mA in this type of LD in our experiment. Therefore the minimum equivalent wavelength Λ becomes ~8.95 mm theoretically. In the direct phase modulation of the LD, however, a large OPD is necessary to satisfy the appropriate modulation depth, $z = 2.45$, with a small modulation current that does not induce the intensity modulation in the interference signal. In our experiment the amplitude of the modulation current and the OPD were 0.44 mA and ~80 mm, respectively. On the other hand, the maximum Λ is unlimited because the wavelength difference Δλ can be set as small as we want. But usually the LD has a finite coherent length, so we cannot lengthen the OPD without limit.

Consequently, the minimum Λ and maximum Λ are restricted by the initial OPD, which is decided by the amplitude of the modulation current, and the coherent length of the LD, respectively, but Λ is very

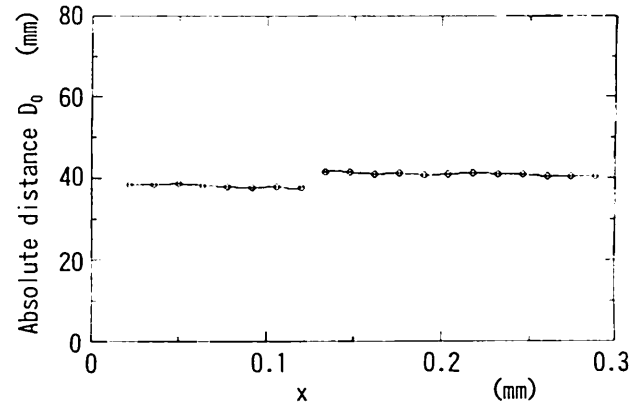

Fig. 7. Measured step height of the block gauge whose thickness was ~2 mm. The measured values are represented by circles.

large compared with that in the other interferometer. The feasible measuring range in distance is then $\Lambda/2$, which is similar to that in the conventional interferometer.

6. Conclusions

A new signal-processing method has been introduced into the wavelength-multiplexed phase-locked LD interferometer. The fundamental error caused by offset voltage can be eliminated in a simple way. The principle and experimental results have been described. The advantage of this interferometer is that there is no need to consider errors caused by offset voltage in the feedback signals. Because only one LD is required in our interferometer, the optical system is very simple despite the use of multiple wavelengths. The measurement error is estimated to be $\sim\Lambda/600$ rms with the experimental measurement.

References

1. J. C. Wyant, "Testing aspherics using two-wavelength holography," Appl. Opt. **10,** 2113–2118 (1971).
2. Y.-Y. Cheng and J. C. Wyant, "Two-wavelength phase shifting interferometry," Appl. Opt. **23,** 4539–4543 (1984).
3. A. F. Fercher, H. Z. Hu, and U. Vry, "Rough surface interferometry with a two-wavelength heterodyne speckle interferometer," Appl. Opt. **24,** 2181–2188 (1985).
4. K. Creath, "Step height measurement using two-wavelength phase-shifting interferometry," Appl. Opt. **26,** 2810–2816 (1987).
5. A. J. den Boef, "Two-wavelength scanning spot interferometer using single-frequency diode lasers," Appl. Opt. **27,** 306–311 (1988).
6. O. Sasaki, H. Sasazaki, and T. Suzuki, "Two-wavelength sinusoidal phase/modulating laser diode interferometer sensitive to external disturbances," Appl. Opt. **30,** 4040–4045 (1991).
7. Y. Ishii and R. Onodera, "Two-wavelength laser-diode interferometry that uses phase-shifting techniques," Opt. Lett. **16,** 1523–1525 (1991).
8. P. de Groot and S. Kishner, "Synthetic wavelength stabilization for two-color laser-diode interferometry," Appl. Opt. **30,** 4026–4033 (1991).
9. C. C. Williams and K. Wickramasinghe, "Optical ranging by wavelength multiplexed interferometry," J. Appl. Phys. **60,** 1900–1903 (1986).
10. T. Suzuki, O. Sasaki, and T. Maruyama, "Absolute distance measurement using wavelength-multiplexed phase-locked laser diode interferometry," Opt. Eng. **35,** 492–497 (1996).
11. G. W. Johonson, D. C. Leiner, and D. T. Moore, "Phase-locked interferometry," Opt. Eng. **18,** 46–52 (1979).
12. H. J. Matthews, D. K. Hamilton, and C. J. R. Sheppard, "Surface profiling by phase-locked interferometry," Appl. Opt. **25,** 2372–2374 (1986).
13. T. Suzuki, O. Sasaki, and T. Maruyama, "Phase locked laser diode interferometry for surface profile measurement," Appl. Opt. **28,** 4407–4410 (1989).
14. O. Sasaki, K. Takahashi, and T. Suzuki, "Sinusoidal phase modulating laser diode interferometer with a feedback control system to eliminate external disturbance," Opt. Eng. **29,** 1511–1515 (1990).
15. T. Suzuki, O. Sasaki, K. Higuchi, and T. Maruyama, "Differential type of phase-locked laser diode interferometer free from external disturbance," Appl. Opt. **31,** 7242–7248 (1992).